The contribution of CASIEL infill walls to the shear resistance of steel frames

Bright M. Ng'andu, Dirk R.W. Martens, Ad T. Vermeltfoort
Eindhoven University of Technology, the Netherlands

In Europe, calcium silicate element (CASIEL) walls are increasingly employed as partitions and external claddings in buildings. The CASIEL infills and the frames mutually interact through frame-wall interfaces. This interaction has a significant influence on the load transmission paths of building structures. In order to safeguard the walls and the frames, as well as the finishes from damages, this behaviour needs to be understood and translated into design guidelines. This paper presents results of experiments conducted on 10 large-scale CASIEL-infilled steel frames monotonically loaded by in-plane shear. Parameters investigated included frame size, rigidity of frame connections, frame-wall interface gaps, and bearing wedges at the frame top-corners. In general, there was an initial stiff load deflection response followed by a much less stiff response during which frame-wall separation occurred and another stiff response leading to, in the majority of cases, diagonal tension cracking in the infill walls. Shear sliding along the top most bed joint was observed in some specimens. The cracking phase was followed by a less stiff phase, but with an increasing load resistance leading to ultimate failure through crushing of the wall. Increasing the size of the bounding frames increased the stiffness of the infilled frames and moderately increased the cracking loads. Initial gaps between the roof beams and CASIEL wall panels resulted in reduced infilled frame stiffnesses during the transition phase, although they did not significantly reduce the cracking loads. By using bearing wedges in the top corners, the influence of the top gaps was practically eliminated. This technique may be significant in developing a construction technique for industrial application of infilled frames. The rigidity of the frame connections did not significantly influence the stiffnesses and cracking loads of the infill panels.

Key words: Infilled frames, calcium silicate elements, stiffness, tensile cracking, shear sliding, crushing

1   Introduction

This article describes and presents results from an experimental research program aimed at developing design guidelines for steel frames infilled with calcium silicate element (CASIEL) walls and subjected to external in-plane loads. The objectives of the research program were to experimentally establish the general behaviour, develop a numerical model, calibrate it and perform parametric studies. Firstly, the key terms 'infilled frames and CASIELs' are defined. Secondly, a description of the experimental technique is given. Thirdly, experimental results are presented before, finally, giving some conclusions.

1.1   Defining 'infilled frames' and 'CASIELs'

Infilled frames can simply be defined as beams and columns confining walls, as shown, for instance, in Figure 1.

Figure 1: Infilled frames - beams and columns confining walls

When the walls are not deliberately isolated from the frame, they interact with the frame producing a structural behaviour that is different from a simple addition of the two components. In a mutually beneficial relationship, the infill wall provides lateral rigidity while the bounding frame provides some ductility. If this interaction is ignored in the design assumptions, the actual stress path in the building may be significantly deviant from the assumptions, and potentially risky. If the composite action is assessed it can lead not only to a safer design but also to lighter frames and connections, which in turn are cheaper.

In the last two to three decades, a new way of building walls, namely with calcium silicate elements (CASIELs) in thin–layer mortar, has evolved (Berkers 1995). Calcium silicate elements are large building 'stones', produced by mixing sand, lime and water, moulding and curing under conditions of pressurized steam, as illustrated in Figure 2. The term 'element' is used to distinguish them or their size from traditional units and blocks. The dimensions of elements are 900 to 1000 mm long, 520 to 650 mm high and 100 to 300 mm thick, and they weigh approximately 100 to 400 kg per piece. As such, they are in the range of 10 to 40 times heavier than ordinary blocks, weighing, say, 10 kg.
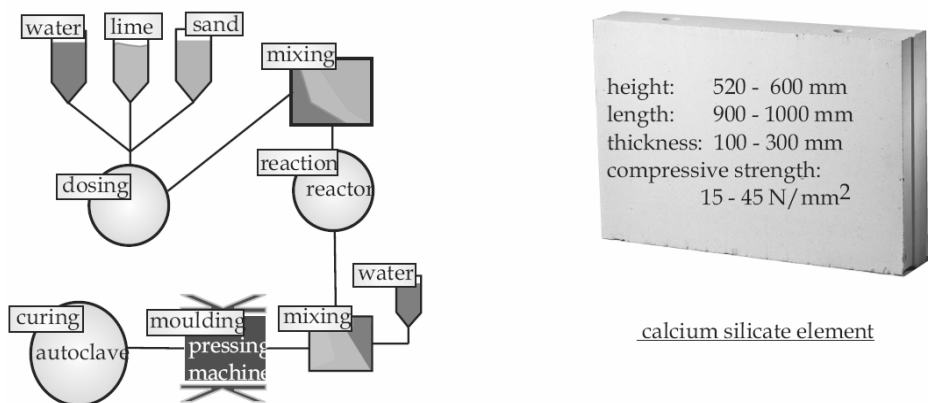
Figure 2: Production process and dimensions of Calcium Silicate Elements

Unlike traditional masonry in which a bricklayer must painstakingly place unit by unit, erecting CASIEL walls involves the use of a small crane. An element is gripped through purpose-inbuilt holes, hoisted and hand guided into position. Its edge, which has a groove, is placed on the 'tongue' edge of the adjacent or preceding element, as shown in Figure 3. Dimensional tolerances and adhesion at the joints are provided through special thin-layer 'mortar'. The typical joint thickness is 2 to 3 mm.

Building with calcium silicate elements has tremendously enhanced the speed of erecting walls while reducing labour costs and the physical stress of the bricklayers on site. Finishing costs are also significantly reduced, due to the smoothness of the surface of calcium silicate elements. Other factors cited in favour of calcium silicate elements include excellent structural performance of the material, environmental friendliness (the material can be crushed and used as earth fill or reused to produce other calcium silicate products after the structure's life span), better quality products due to production of elements in

factory controlled conditions and possibilities of construction during cold/rainy weather conditions.
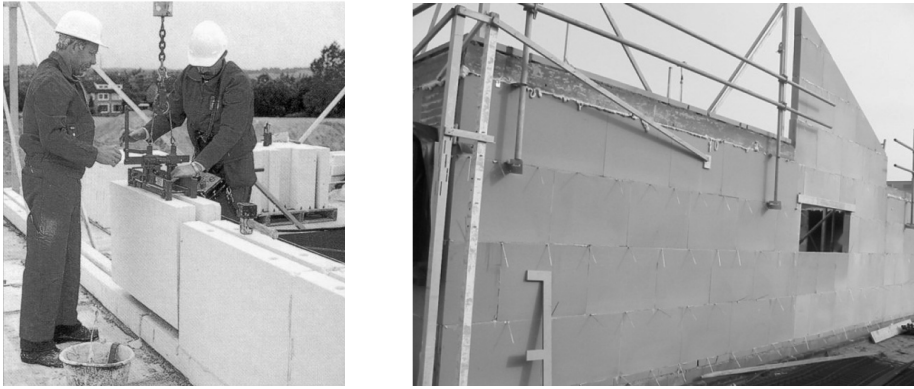
Figure 3: Building walls with CASIELs

1.2 *CASIEL- infilled frames*

Although a lot of research has been done on infilled frames in the past, there has not yet been any research involving infill walls constructed from CASIELs. Most full - scale experiments have been on frames infilled with clay or concrete brick masonry (e.g. Dawe & Seah, 1989; Dhanasekar, 1985; Moghaddam, 2004; El-Dakhakhni et al., 2006). Scale model tests using micro-concrete have also been done (Stafford-Smith, 1966; Kadir & Hendry, 1975).

While similarities may be expected between the behaviour of CASIEL walls and traditional brick masonry infills, significant differences might also occur. The major difference in the two types of walls is that the former has much fewer and much thinner joints than the latter. Depending upon the scale at which the wall is regarded, either of the wall types may be seen as more homogenous than the other. From a global point of view, a masonry wall, with small bricks, may be seen as a 'homogenous' composite while a CASIEL wall is an articulation of large blocks with discontinuities at the thin-layer joints. On the other hand, at a local level, CASIELs may be taken as homogeneous (and isotropic) while brick walls appear as a heterogeneous articulation of bricks and mortar through discrete interfaces.

A second peculiarity of CASIEL walls has to do with the construction process. By virtue of the size of the elements and the handling equipment, some working space, as illustrated in Figure 4, is required to fit in the last CASIEL row below the roof beam. The result is that initial gaps are left between the frame and the wall. This difficulty in achieving a snug contact between the wall and the frame results in boundary incompatibilities, which, coupled with

204

shrinkage, deserve special attention in the modelling and design of the structure. If the walls must participate in carrying the load, construction techniques and details must be developed to ensure predictable transfer of stresses across the frame-to-wall interface. Conversely, if it is assumed that infill walls do not participate in carrying loads, details which match this assumption must be realised.
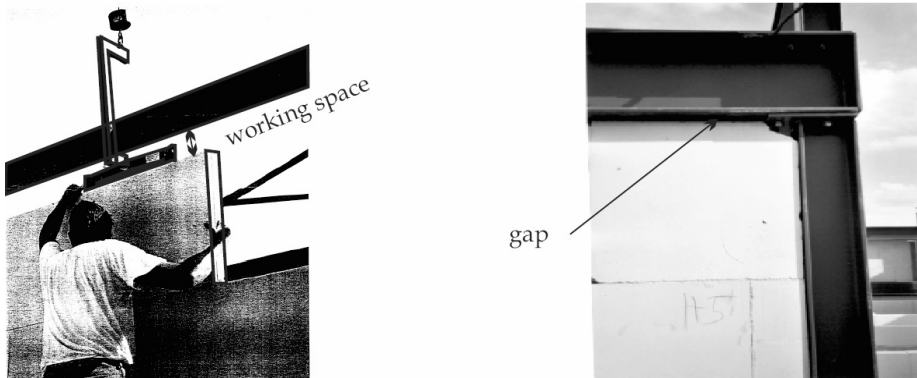
Figure 4: Infilling frames with CASIELs, leaving boundary gaps

1.3   *Description of Experiments*

In this investigation large - scale experiments were used to observe and measure the response of steel frames infilled with CASIEL walls to in-plane monotonic loading. Theoretically, steel frames contribute ductility and infill walls contribute stiffness to infilled frames. The infill wall acts as a diagonal brace to the frame. The effectiveness of the diagonal brace depends upon the frame-to-wall stiffness ratio, the contact, bond and shear characteristics at the frame-wall interface and the strength of the infill under biaxial loading (reference). In this study the influence of the following factors was investigated: (a) a structural configuration factor: the frame-to-wall stiffness ratio, (b) an interface detail factor: a gap below the roof beam, and (c) a construction technique: the use of a corner bearing wedge.

1.3.1   *Tests apparatus*

A testing apparatus was required for the purpose of providing a platform for the specimen and applying in-plane loading. The basic requirements of such an apparatus have to do with the way the apparatus interacts with its own support, normally the structural floor, and the way it interacts with the specimen at the specimen supports and point of load introduction.

Several testing arrangements for achieving the above purpose are found in the literature. Typically this involves a rigid frame anchored to a ground beam or structural floor. A jack is placed between the rigid frame and the specimen. The reaction force from the specimen is transmitted to the ground support through the rigid frame.

In this project, a purpose designed reaction frame was used as a platform to mount and load the specimens. The key characteristics of the reaction frame are: the provision for large scale specimens, the non-reliance on a structural floor and necessarily, the sufficient rigidity.

A schematic concept of the reaction frame is shown in Figure 5. The reaction frame is composed of twin triangular frames, one on either side of the specimen, and connected through rigid steel members at its vertices. The members of the twin triangular reaction frames were made out of European HE 300 B profiles. The links between the twin rigid frames provide support points for the specimen and the loading jack.

At Support A, (Figure 5) this connection is by means of a heavy steel block. The steel block is bolted to the stiffened flanges of the triangular frames. The specimen rests on this block of steel so that the specimen is restrained from in-plane horizontal and vertical displacement. In this way, for evaluation of the behaviour of the structure, this support is modelled as a pin support.
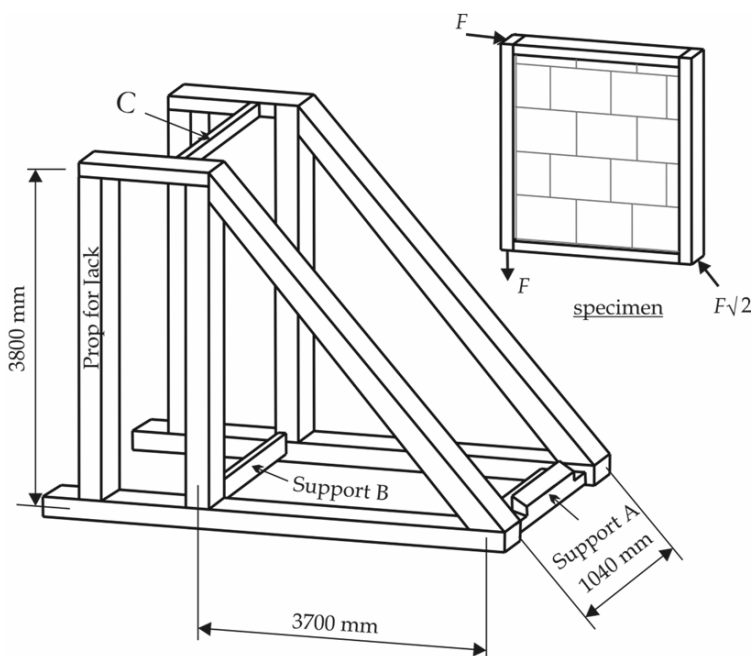
Figure 5: Schematic view of reaction frame and specimen

At Support B, a stiff steel beam is bolted to the triangular frames. Two types of Support B were used during the investigation. In the first type, shown in Figure 6a and used for the first four tests, denoted as Test 1 to 4, a slender steel plate was bolted to the reaction frame at the bottom and the specimen above. In the second type, shown in Figure 6b and used in the last six tests, denoted as Test 5 to 10, four steel rods were used to tie the reaction frame to the specimen. The slender plate or the steel rods used at Support B were intended to provide high vertical restraint and as low horizontal restraint as possible. In this way, for evaluation of the behaviour of the structure, B would be modelled as a roller support. At the top vertex of the reaction frame, another stiff steel plate, C, spans across the two triangular frames. It is on this steel plate that the 2 MN jack was supported. Figure 7 depicts the test arrangement with a specimen mounted (slotted in).
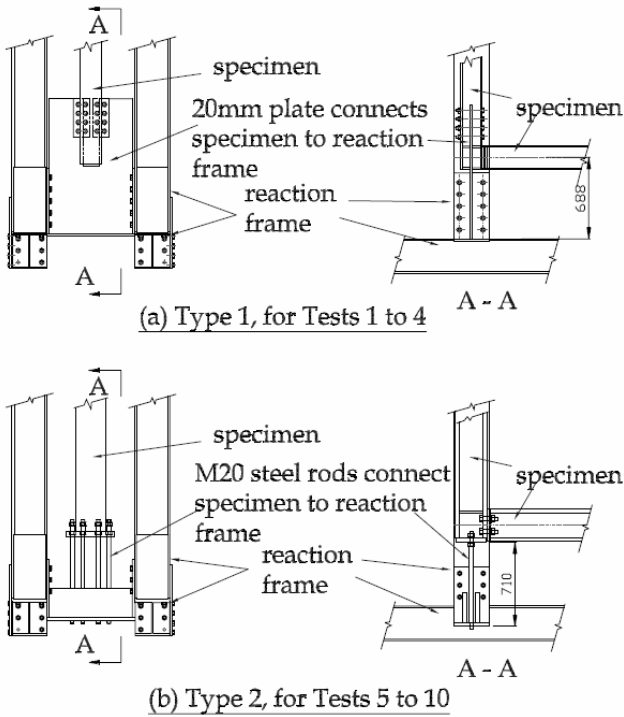
Figure 6: Connection of the frames to Support B

Once a force is applied to the specimen, the jack pushes against the steel plate and the reaction force is transferred to the reaction frame. The insert in Figure 5 shows the forces acting on the infilled frame. The slanting members of the reaction frame share the tension

while the vertical members bear the compression. A simple elastic analysis showed that with an ultimate jack force of 2 MN, strains in the reaction frames will be, insignificantly, in the order of 0.1 mm/m, representing stresses less than 10% of yield strength. Thus, for the level of loads attained in this testing programme, the reaction frame is sufficiently rigid and therefore able to absorb or release energy from the specimen without undergoing significant deformations.
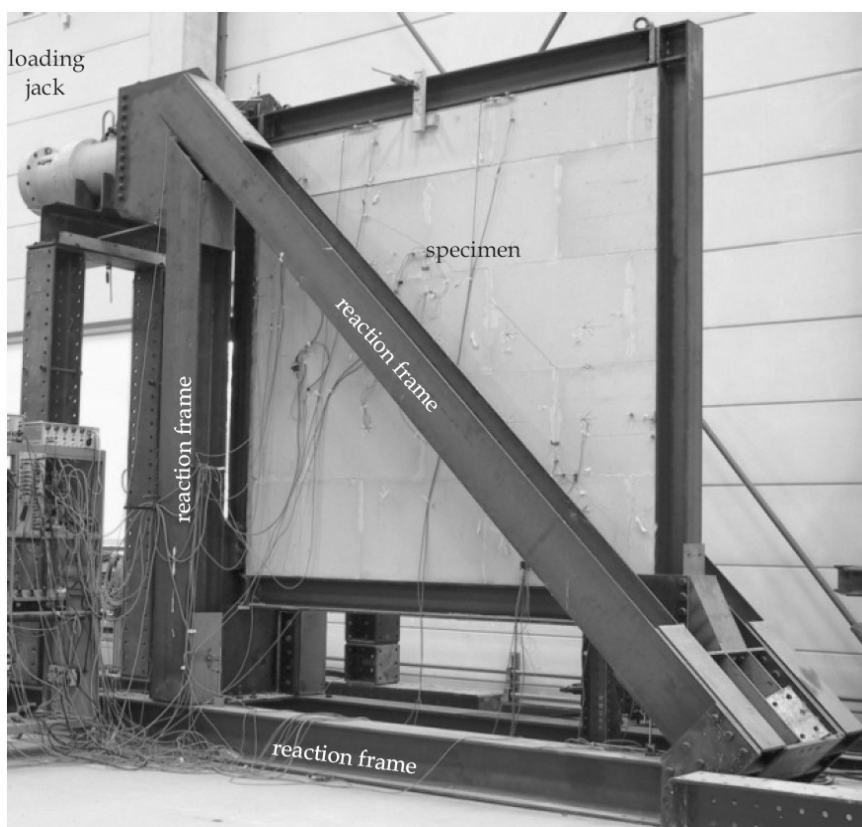
Figure 7: Test arrangement with mounted specimen

The monotonic load was applied by a hydraulic jack mounted at roof level of the specimen. The jack piston was 210 mm in diameter. At the end of the jack piston a 220 mm deep by 300 mm wide by 80 mm thick loading plate was fixed. The purpose of this loading plate was to uniformly spread out the applied load over the specimen column flange width. With a thickness of 80 mm, the loading plate was stiff enough to ensure negligible bending of the loading plate, thus achieving uniform displacement over the loading area. Further,

208

the loading plate was fixed to the jack piston in such a way that it could tilt about the axis of the ram by gliding over a spherical seating, allowing it to press parallel onto the specimen surface. Once the loading surface was pressing parallel on the specimen surface, friction between the spherical seat and the loading plate would maintain its inclination. A description of this type of spherical seat and loading plate according to the requirements of ASTM E447-84 (1984) is given by Drysdale et al. (1999).

1.3.2 Specimen types

Each infilled frame was nominally 3000 mm by 3000 mm. Steel I-sections, with semi rigid bolted connections were used for the bounding frame. The infill walls were constructed from 897 mm x 594 mm x 150 mm CASIELs in thin-layer mortar. Five different types of specimens, in duplicate, were used. Figure 8 and Table 1 show the main characteristics of the specimens, namely: (a) strong or weak frames; (b) frames with or without gaps, and; (c) frames with corner bearing wedges.

Weak frames were constructed from HE 200 B sections (moment of inertia about main axis, I_X = 5696 x 10^4 mm^4) for beams and HE 180 B sections (I_X = 3831 x 10^4 mm^4) for columns. For each connection, a 15 mm thick beam end plate was bolted with four M20 bolts to the column flange. The strong frames were constructed from HE 240 M (Ix = 24290 x 10^4 mm^4) steel sections all round. Beam end plates of 30 mm thickness were bolted to stiffened column flanges. Back plates of 15 mm thickness were welded to the column flange. Tests of the stiffness of bare frames showed that the strong frames, at an average of 9.2 kN/mm were 3 times stiffer than the weak frames, at an average of 3.1 kN/mm.

1.3.3 Corner bearing wedges

When fitting an infill wall into a frame, tolerance gaps remain between the edges of the wall and the surrounding frame. Gaps may also be caused by shrinkage of the infill wall. In these experiments, the behaviour of infilled frames with weak frames with and without gaps between the top of the infill wall and the roof beam was compared. A comparison was also made between infilled frames with strong frames with corner bearing wedges with and without gaps. For Specimen Type 1, the 12 mm gap between the wall and the roof beam was packed with ordinary mortar while, for Specimen Type 2 an open gap was left. Observations of other researchers, which have now been corroborated by results from the current research, indicated that the presence of interface gaps reduces the stiffness of infilled frames during the early stages of loading. This is because of a delay in interlocking

of the wall and frame, causing large deflections at this stage. Closing interface gaps by packing mortar, as was done in this research, is a slow process and does not guarantee consistent filling of the gap. In order to eliminate the negative influence of the top gap and at the same time to remove the necessity of filling it with mortar, a novel construction

Specimen Type 1   Specimen Type 2

Specimen Type 3   Specimen Type 4   Specimen Type 5
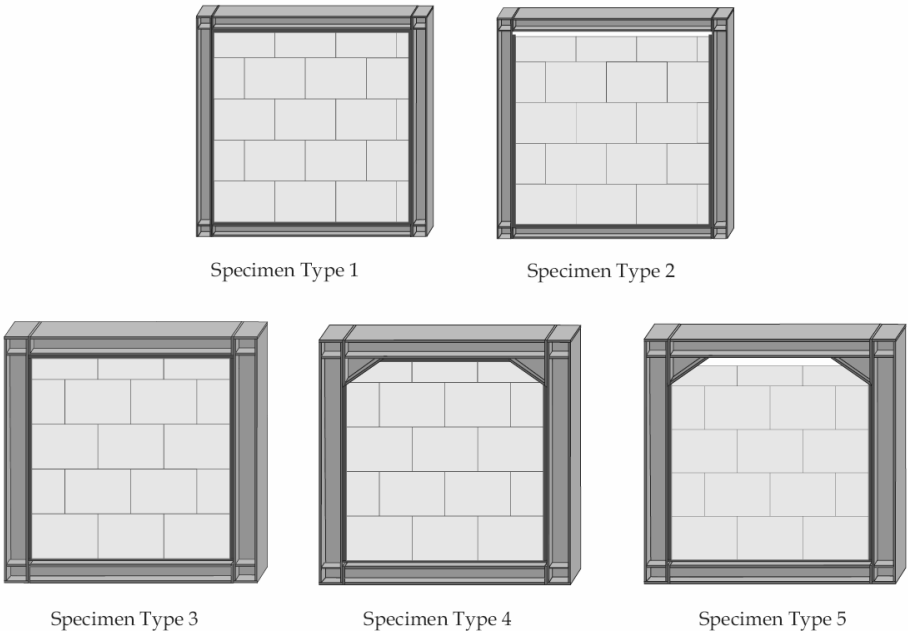
Figure 8: Specimen types

Table 1:   Types of infilled frame specimens

Specimen Type	TEST No	Beam Section	Column Section	Wall Thickness (mm)	Gap Below Roof Beam (mm)	Bearing Wedge
1	1 & 2	HE200B	HE180B	150	Nil	Nil
2	3 & 4	HE200B	HE180B	150	12	Nil
3	5 & 6	HE240M	HE240M	150	Nil	Nil
4	7 & 8	HE240M	HE240M	150	Nil	Present
5	9 & 10	HE240M	HE240M	150	12	Present

technique was investigated. The basic idea of the technique was to improve the contact between the frame and the wall at the frame corners. This was investigated by the use of Specimen Type 4 and Specimen Type 5. In Specimen Types 4 and 5, triangular corner bearing wedges were bolted to beam and column flanges at the top corners of the frames. The surfaces of the flanges were the bearing surfaces through which the load would be transmitted into the infill wall.

In order to place the CASIELs against these bearing wedges, the steps illustrated in Figure 9 were followed. Firstly, the top layer of CASIELs was laid, leaving a void in the middle. Next, one wedged piece, cut out of a CASIEL, was inserted into the void. Finally, by pushing the second wedged piece of a CASIEL downwards, CASIELs in that row were pushed sideways against the corner bearing wedges. The only difference between Specimen Type 4 and Specimen Type 5 was that the top gap was packed with mortar in the former and left open in the latter.
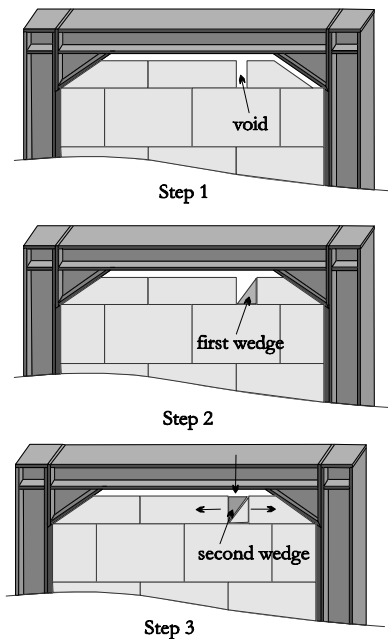
Figure 9: Pushing CASIELs sideways
against steel using wedges
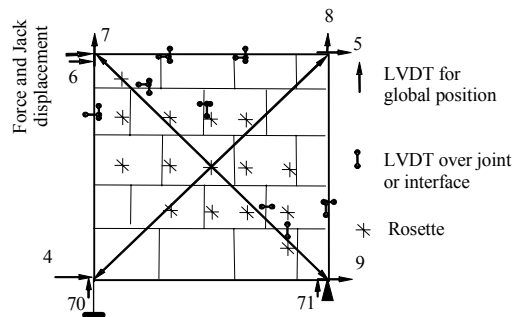
Figure 10: Measurement scheme

1.3.4 Measurements

Figure 10 shows the arrangement of Linear Variable Displacement Transducers (LVDTs) and rosettes on the specimen. The position of the specimen in relation to the ground was measured by LVDTs as indicated by the numbers 4, 5, 6, 7, 8, 9, 70, and 71 at the corners of the specimen. These LVDTs were fixed to a separate measuring frame. In order to decipher the strain distribution in the wall, rosettes were placed on a 500 mm by 500 mm grid on the wall. The grid was arranged with a bias to cover the area along the compression diagonal since most of the deformations were expected to take place there. Gaps and slip at the frame-to-wall interface as well as across and along joints in the wall were measured by LVDTs at specified points. The applied force and displacement of the loading cylinder head were also measured by inbuilt strain gauges and LVDTs respectively. A deformation-controlled load was applied, at 1 mm/min, using the 2 MN hydraulic jack mounted at roof beam level.

2   Experimental results

2.1   *Overview of load deformation responses*

A load deflection graph, shown in Figure 11, from the results of Test 5, is hereby used to typify the behaviour of the infilled frames tested. The stiffening effect of the wall on the bare frame is self evident. The bare frame used in Test 5 had a stiffness of 9.8 kN/mm.
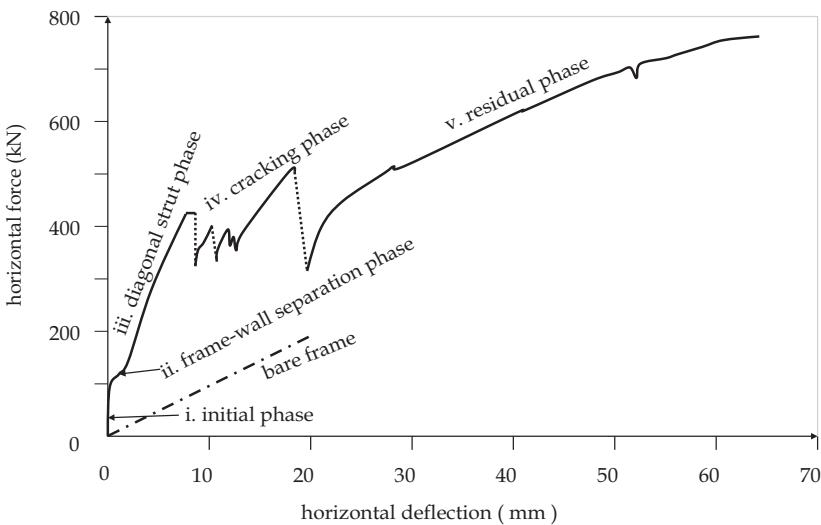
Figure 11: Typical load deflection behaviour, from Test 5

(This was measured only up to a deflection of 5 mm; it is extrapolated up to 20 mm in Figure 11). A deflection of 7.6 mm, that is, at the onset of the cracking phase, corresponds with a load of 409 kN for the infilled frame. The secant stiffness of the infilled frame at that point is 54 kN/mm. That represents a 5.5 times increase in the stiffness on account of the infill wall. Similar comparisons between stiffnesses of the other bare frames and secant stiffnesses of corresponding infilled frames at the onset of the cracking phase are presented in Table 2. These results show that addition of infill panels increased the stiffness of frames between threefold to tenfold. The least increase was in the cases of Test 3 and Test 4 which were weak frames with gaps between the roof beams and the walls. The stiffnesses for these frames are particularly low due to the influence of the frame-to-wall gaps.

Table 2: Comparison between bare frame and infilled frame stiffnesses

| Specimen Type | Test | Stiffness (kN/mm) | | factor increase in stiffness |
		Bare frame	infilled frame*	
1	1	2.9	25	8.6
	2	3.5	22	6.3
2	3	3.3	12	3.6
	4	3.4	16	4.7
3	5	9.8	54	5.5
	6	8.5	65	7.7
4	7	10.7	61	5.7
	8	12.1	100	8.3
5	9	17.7	139	7.9
	10	11.9	114	9.6

*secant stiffness of infilled frame at onset of cracking

Figure 11 further shows that the response of the infilled frames can be categorized in five stages, namely, an initial phase, a frame-wall separation phase, a diagonal strut phase, a cracking phase and a residual strength phase. During the initial phase the bounding frame and the infill wall act as one composite 'shear element'. The infilled frame is, at this stage, very stiff. At the end of this initial stage, typically within the first 0.3 mm of load point horizontal deflection, the wall separates from the bounding frame, with the gap propagating from the tension corners. The wall adjusts in position within the bounding

frame. In general the gap between the wall and the frame members extended more than three quarters of the length or height of the infill panels.

This 'frame-wall separation' phase was accompanied by a temporal drop in the stiffness, and in some cases, in the load carried by the frame. The frame-wall separation phase was succeeded by a structural configuration in which the wall, being locked with the frame at the loaded corners, acted as a diagonal strut in the frame, thus, the 'diagonal strut phase'. In this phase, the load deflection response was typically a linear curve, although its slope was less than that of the initial phase. Diagonal strutting led to a cracking phase. A big crack more or less parallel to the compression diagonal suddenly appeared, accompanied with an explosive bang, and as much as a 30% drop in load. The diagonal crack cut through the CASIELs and the joints. In some cases, a shear crack occurred along the uppermost bed joint prior to the diagonal crack. Such a shear crack led to a drop in the load although the stiffness of the infilled frame was almost immediately recovered. With increased deflection, more diagonal cracks appeared. Figure 12 shows examples of cracked specimens. A residual phase followed in which the infilled frame carried increasing loads, albeit at a much reduced stiffness. Crushing at the loaded corners and some junctions between header and bed joints occurred as the load became more or less constant. At this point the test was stopped.
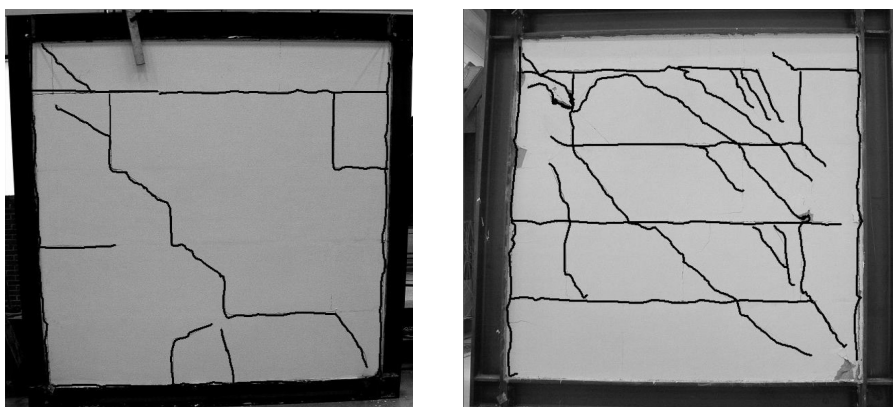
Figure 12: Cracking patterns, photographs from Test 1 and Test 5

2.2   *Principal stress distributions*

In order to configure the geometry of the diagonal strut formed by the wall, it is desirable to evaluate the distribution of strains and stresses in the wall. In these tests, strains were measured by rosettes arranged in a 500 mm x 500 mm grid. Principal strains can be derived

through an analysis of a two dimensional stress state (Ng'andu, 2006). Using the principal strains, the stresses can be estimated for known values of the elastic modulus, E, and Poisson's ratio, υ. Auxiliary tests (Vermeltfoort & Ng'andu, 2005) showed that the stress-strain relationships of the CASIELs were practically linear up to 95% of the maximum stress. The values of the elastic modulus and Poisson's ratio for the CASIELs were determined as 6000 N/mm² and 0.2 respectively. The principal strains and stresses so derived were plotted at the various measuring points on the walls. In Figure 13, for instance, the principal stresses for Test 5 are plotted along the compression diagonal. (It should be born in mind that these major stresses are not necessarily in the same direction). The pattern of principal stress distribution shows the following:

1. There is a concentration of compressive principal stresses in the proximity of the loaded corners. This is graphically seen in Figure 13a. The highest compressive principal stress for a load of 400 kN was 6.36 N/mm² at the measuring point near the loaded corner. Since the crushing strength of the CASIELs was higher than this, (in the order of 15 N/mm²), crushing, at this stage was not observed

2. Tensile principal stresses are higher in the central region of the wall. This is graphically shown in Figure 13b. The tensile stress recorded at the centre of the infill panel for a load of 400 kN was 0.83 N/mm².

3. The regions near the loaded corners are in biaxial compression while the central regions of the wall are subjected to compression and tension. Tensile stresses led to diagonal tensile cracking.

4. With respect to the distribution of stresses across the compression diagonal (i.e. along the tension diagonal), Figure 14a profiles the major and minor principal stresses. Both compressive and tensile principal stresses are pronounced at the centre of the infill panel and diminish along the tension diagonal.

From the foregoing discussion on stress distributions in the infill panels, and with regard to the configuration of the diagonal strut formed by the infill wall, it is evident that the compression band is narrow near the loaded corners and wide (bulging) at the centre. For visualization, the shape of the diagonal strut can be portrayed as shown in Figure 14b. In Figure 14a a linear distribution of stresses between the measuring points is assumed. More measurement points would be required to show the actual profile of stress distributions.

However, if a triangular distribution over the whole length of the tension diagonal is assumed, the diagonal compressive force F_d, can be estimated from equation (1).

$$F_d = \frac{1}{2}\sigma_{max}\, l_d\, t$$

(1)

where: σ_{max} is the compressive stress at the centre of the infill wall,

l_d is the diagonal length of the infill wall, and,

t is the thickness of the infill wall.

• measuring point

—··— at 50 kN   ------- at 300 kN

— · — at 200 kN   —— at 400 kN

(a) major principal stresses   (b) minor principal stresses
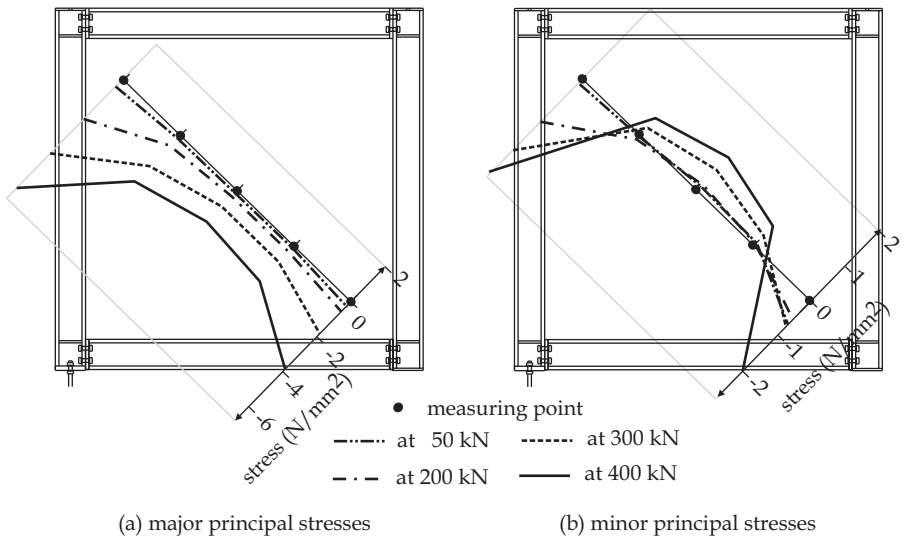
Figure 13: Principal stresses along compression diagonal

For Test 5, as an example, the compressive stress at the centre of the panel, just before cracking was 1.89 N/mm^2. With a diagonal length of 4200 mm and wall thickness of 150 mm, the diagonal force determined with equation (1) is 595 kN. The horizontal component of this force is 420 kN, which compares well with the measured cracking load of 400 kN. Considering, though, the fact that the direct resistance of the frame is ignored in this approximation, it can be said that a triangular stress distribution curve across the compression diagonal overestimated the diagonal force. It is reasonable to suggest that the distribution of stress across the diagonal is more or less in the shape of a Gauss curve, Figure 14b. It is expected that the characteristics of the Gauss curve are a function of the contact lengths at the frame-infill interface and the geometry of the infill wall.

· measuring point

—·— at 50 kN ----- at 300 kN
—··— at 200 kN —— at 400 kN

(a) principal stresses

(b) triangular or Gauss curve stress distribution profile
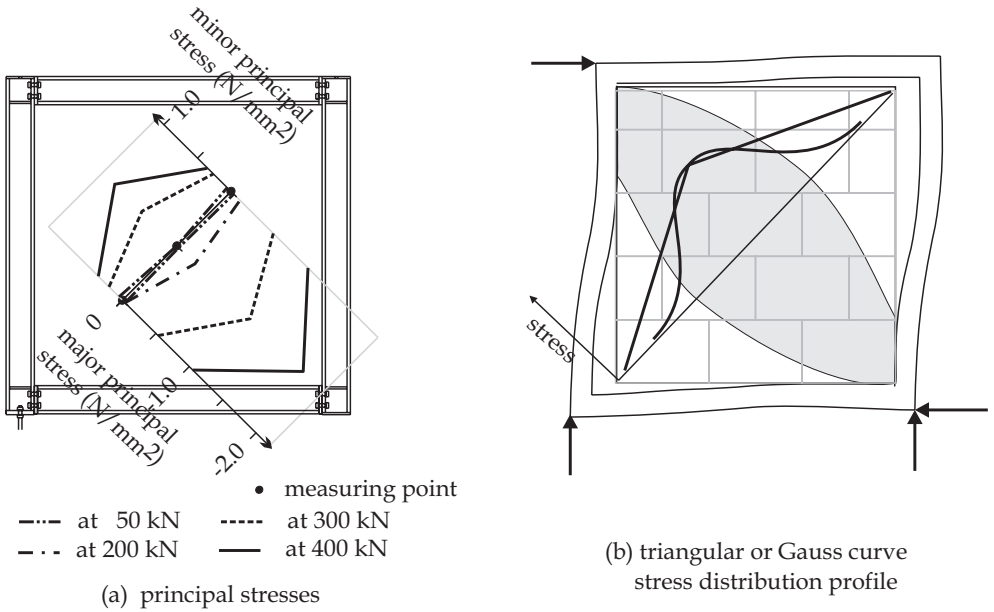
Figure 14: Principal stresses across compression diagonal

2.3 *Influence of frame stiffness*

One of the parameters of interest is the change in strength and stiffness of an infilled frame that is associated with an increase in the sizes of the frame members. On average the experimental stiffness of the light bare frames was 3.1 kN/mm. The strong frames on the other hand were constructed from HE 240M profiles and the stiffness of the bare frames were, on average 9.2 kN/mm. Figure 15 shows load deflection responses for four tests. Frames for Test 1 and Test 2 were of the weak frame type while those for Test 5 and Test 6 were of the strong type. The responses of the two frame types are compared below.

Increasing the frame stiffness increased the stiffness of the infilled frames. For purposes of comparison, the slope of each load deflection graph in the more or less linear diagonal strutting phase, herein after referred to as the primary stiffness, was calculated. The primary stiffnesses as well as the values of the load at which the first major cracks appeared are shown in Table 3. With a threefold increase in the frame stiffness, the primary stiffness of the infilled frames increased by a factor of 1.5.

Figure 15 and Table 3 further show that increasing the frame stiffness also increased the load at which the first major (diagonal) cracking occurred. Increasing the frame stiffness from 3.1 kN/mm to 9.2 kN/mm resulted in an increase in the (average) major cracking load from 284 to 409 kN, i.e., a difference of 125 kN. Although this increase is expected by
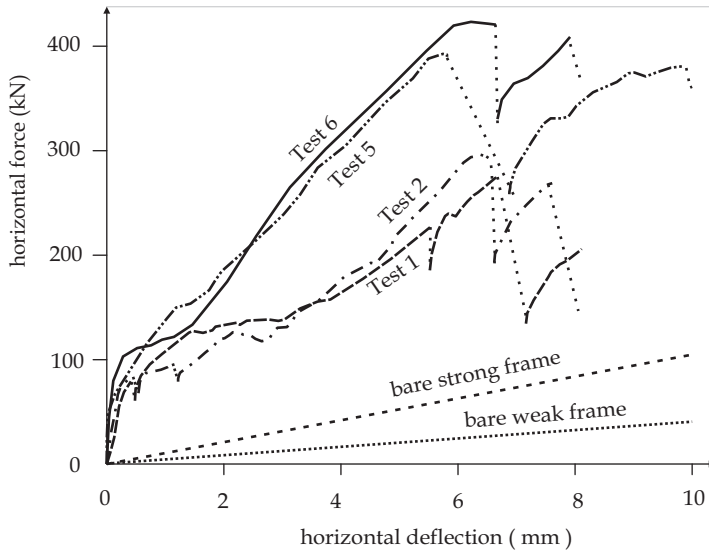
Figure 15:   Influence of the stiffness of the bounding frame

Table 3:   Stiffnesses and cracking loads for Specimen Types 1 and 3

Specimen Type	Test	Primary Stiffness	Average Primary Stiffness	Shear Slip Load	Diagonal cracking load	Average diagonal cracking load
		(kN/mm)	(kN/mm)	(kN)	(kN)	(kN)
1	1	42	41	not observed	293	284
	2	39		235	275	
3	5	54	59	not observed	409	400
	6	63		not observed	390	

virtue of the higher load resisted by the stiffer bare frame, the increase is not, per se directly proportional to the increase of the bare frame stiffness. For instance, at a deflection of 7 mm, which is the deflection at about which the stronger frame specimens cracked, the difference in loads resisted by the weak bare frame, of stiffness 3.1 kN/mm, and bare strong frame of stiffness 9.2 kN/mm would be 42.7 kN. As stated earlier, in Figure 15 the corresponding difference in the load resisted by the infilled frames is in the order of 125 kN.

This disproportionate increase in the stiffness and strength of the infilled frame cannot be accounted for by the simple additional stiffness of the frame. As asserted by many

218

researchers, the possible explanation may be in the increased composite action that results from increased contact area at the frame-wall interface. This would lead to a wider distribution of stress and a higher failure load.

 It can also be seen from Figure 15 that the specimens with the stronger frames had shorter and smoother transition phases while those with weaker frames had longer, if jagged, transition curves. This can be attributed to a firmer confinement of the infill panel, in the case of stronger frames, thereby reducing the rate of energy changes in the structure during the process of frame-wall separation.

It is further noted that for Test 2, a shear crack appeared along the top most bed joint, at a load of 235 kN, prior to the appearance of the diagonal crack. Presumably, the shear crack occurred due to a poor filling of the mortar joints in this specimen. Once the crack along the bed joint below the topmost CASIEL layer occurred, the infilled frame, more or less instantly, recovered its stiffness.

2.4   *Influence of gaps*

The influence of initial gaps between the upper beams and the infill panels is plainly evident in Figure 16. In the four tests depicted, the bounding frames were nominally identical. Specimens for Test 3 and Test 4, however, had 12 mm initial gaps between the upper beams and the infill panels. Due to the gaps, there was a large deflection range in which the tangent stiffnesses of the infilled frames were essentially equal to those of the bare frames. During this range the walls glided within the boundary frame until they could establish a locking position with the bounding frames in the region of the loaded corners. Once in that position,
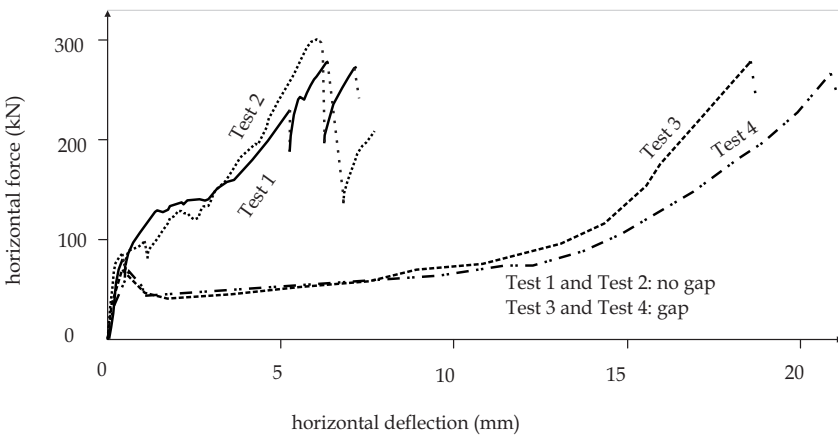
Figure 16: Influence of gaps between upper beam and infill wall

Table 4: Stiffnesses and cracking loads for Specimen Types 1 & 2

Specimen Type	Test	Primary Stiffness	Average Primary Stiffness	Shear Slip Load	Diagonal cracking load	Average diagonal. cracking load
		(kN/mm)	(kN/mm)	(kN)	(kN)	(kN)
1	1	42	41	not observed	293	284
	2	39		235	275	
2	3	29	33	not observed	270	278
	4	36		285	285	

the walls acted as bracing struts in a similar way to infilled frames without initial gaps. It can be seen in Table 4 that the average stiffness of Type 2 specimens, which is 33 kN/mm, was 20% less than 41 kN/mm for Type 1 specimens. The difference is attributed to the fact that initial frame-to-wall gaps led to shorter frame-to-wall contact lengths compared to specimens without gaps.

2.5 *Effect of corner bearing wedges*

The effect of using corner bearing wedges on infilled frames with gaps between the upper beams and the infill panels can be seen in Figure 17 and in Table 5.

In the initial phase Type 5 specimens, Test 9 and Test 10, resisted higher loads before the transition phase than Type 4 specimens, Test 7 and Test 8. It was observed that in Test 9 and Test 10, separation of the wall from the frame properly occurred at a higher load of approximately 130 kN as compared to approximately 70 kN for Test 7 and Test 8. Secondly, infilled frames with a corner bearing wedge and a gap were stiffer than infilled frames without an initial gap. A clear cause for this increase in the separation load and in primary stiffness could not be identified. A study of the strength characteristics of the mortar and CASIELs used did not reveal variations that could explain the difference. It is suspected that in assembling the bare frames, there was a difference in the tightness of the bolt connections which yielded a stiffer bare frame in Test 9 (18 kN/mm, see Table 2). Test 10, whose behaviour is similar to Test 9, however had a bare-frame stiffness similar to Test 7 and 8. The difference in the tightness of the bolt connections, therefore, does not explain the unexpected higher stiffness of the infilled frames in Tests 9 and 10.

It is clear however that the very flexible transition phase associated with frame-to-wall gaps, as observed in Test 3 and Test 4, was eliminated in Test 9 and Test 10. It is, here, assumed that without corner bearing wedges, the influence of initial gaps in weak frames and strong frames is similar. It was further observed that infilled frames with corner bearing wedges and initial gaps had a similar major cracking mode (diagonal tension) and cracking load compared to infilled frames with corner bearing wedges, without initial gaps.
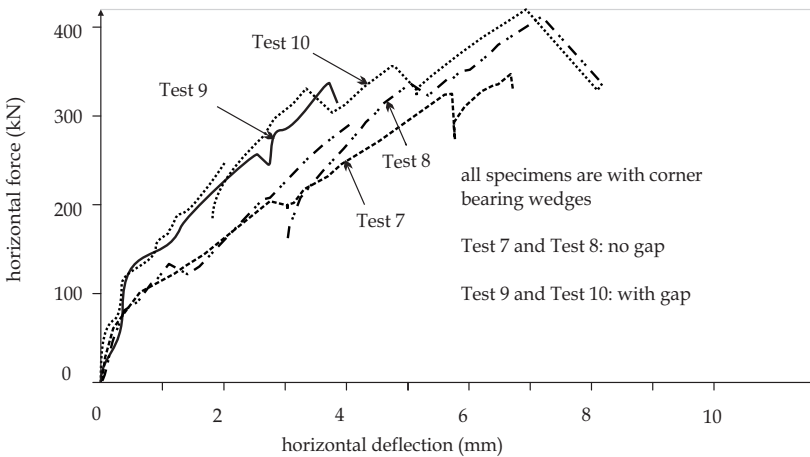
Figure 17:   Influence of gaps on behaviour of infilled frames with corner bearing wedges

Table 5:   Stiffnesses and cracking loads for Specimen Types 4 and 5

Specimen Type	Test	Primary Stiffness (kN/mm)	Average Primary Stiffness (kN/mm)	Shear Slip Load (kN)	Diagonal cracking load (kN)	Average diagonal. cracking load (kN)
4	7	50		340	365	
	8	63	57	not observed	430	398
5	9	74	75	350	370	365
	10	75		290	360	

The final observation is that Test 7 and Test 8, although of the same specimen type, had notable differences in stiffness and diagonal cracking loads. The difference underlines the

statistical nature of masonry due to the variations in material properties and workmanship.

3 Conclusions

Ten large-scale steel frames infilled with CASIEL walls were subjected to in-plane monotonic horizontal loads at roof beam level. The variables investigated were the frame stiffness, the presence or absence of an initial gap below the upper beam, and the influence of top corner bearing wedges.

Analysis of rosette measurements showed that the stresses are concentrated near the loaded corners and spread out at the centre of the infill panel. Load-deformation curves showed an initially high stiffness which transited into a less stiff linear primary stiffness. The deflection range in which the transition took place was longer for infilled frames with a top gap and without a corner bearing wedge. During this transition, the wall separated from the frame at the two tension corners and adjusted within the frame until it was firmly locked up at the compression corners. In all specimens, major cracking occurred by sudden formation of diagonal cracks cutting through the CASIELs and also following the joints. Shear cracking along the topmost bed joint was observed in some specimens, although when this happened, the frames almost instantly recovered their stiffness. Increasing the stiffness of the frames led to an increase in both the infilled frame stiffness and the diagonal tension cracking load.

Results from this investigation strongly indicate that a relatively simple construction technique using CASIEL wedges to push the other CASIELs outwards effectively establishes good contact at the frame-wall interface. A good contact near the loaded corners eliminates the negative influence of a construction gap between the roof beam and the infill wall and consequently eliminates the necessity of packing the gap with mortar. This can lead to improved structural efficiency as well as time/cost effectiveness. Further tests should be conducted to clarify the surprising higher stiffnesses of tests with bearing wedges with gaps than those of similar infilled frames without gaps. It is also recommended that further investigation into the possibility of making the corner bearing wedges out of materials other than steel, possibly CASIELs themselves, is required.

References

American Society of Testing and Materials (1984), Compressive Strength of Masonry Assemblages, *ASTM E447-84*, Philadelphia, PA, USA..

Berkers, W.G.J. (1995) 'Building with calcium Silicate elements' in *Proceedings of the 4th International Masonry Conference*, vol. 1 (7), pp. 176-177.

Dawe, J.L & Seah, C.K. (1989) 'Behaviour of masonry infilled steel frames' in *Journal of the Canadian Society of Civil Engineering*, vol.16, pp. 865-875.

Dhanasekar, M & Page, A.W. (1986) 'The influence of brick masonry infill properties on the behaviour of infilled frames' in *Proceedings of the Institute of Civil Engineers* 81(2), pp. 593-606

Drysdale, R. G., Hamid, A. A. & Baker, L. R. (1999), *Masonry Structures: Behaviour and Design*, *Second Edition*, The Masonry Society, Boulder, Colorado.

El-Dakhakhni, W.W., Hamid, A.A., Hakam, Z.H.R. & Elgaaly, M. (2006) 'Hazard mitigation and strengthening of unreinforced masonry walls using composites' in *Journal of Composite Structures*, vol. 73, (4), pp. 458-477.

Kadir, R. & Hendry, A.W. (1975) 'The behaviour of brickwork infilled frames under racking loads' in *Proceedings of the 5th International Symposium on Load Bearing Brickwork*, British Ceramic Research Association, London, pp. 65-77.

Moghaddam, H.A. (2004) 'Lateral load behaviour of masonry infilled steel frames with repair and retrofit' in *Journal of Structural Engineering,* ASCE, vol. 130(1), pp. 56-63.

Ng'andu, B, M. (2006) *Bracing steel frames with calcium silicate element walls*, PhD Thesis, Eindhoven University of Technology, Eindhoven, The Netherlands.

Stafford-Smith, B. (1966) 'Behaviour of square infilled frames' in *ASCE Journal of the Structural Division*, vol. 92 (ST1), pp 381-403.

Vermeltfoort, A.T. & Ng'andu, B.M. (2005) 'The Response of Calcium Silicate Element Wallettes to 2D Compression Loading' in *Proceedings of the 10th Canadian Masonry Symposium*, Banff, Alberta, Canada.